RESEARCH ARTICLE

Differential interactions of ToLCNDV with different betasatellites reveal complex viral dynamics in *N. benthamiana*

Zafar Iqbal[1☯*], **Muhammad Shafiq**[2☯*], **Sajed Ali**[2], **Mudassar Fareed Awan**[2], **Muhammad Farhan Sarwar**[2], **Imran Amin**[3], **Muhammad Shafiq Shahid**[4], **Rob W. Briddon**[3]

1 Central Laboratories, King Faisal University, Al-Ahsa, Saudi Arabia, **2** Department of Biotechnology, University of Management and Technology, Sialkot Campus, Sialkot, Pakistan, **3** Agricultural Biotechnology Division, National Institute for Biotechnology and Genetic Engineering, Faisalabad, Pakistan, **4** Department of Plant Sciences, College of Agricultural and Marine Sciences, Sultan Qaboos University, Al-Khoud, Muscat, Oman

☯ These authors contributed equally to this work.
* zafar@kfu.edu.sa, zafariqbal2009@gmail.com (ZI); shafiq.4721@gmail.com (MS)

Abstract

Tomato leaf curl New Delhi virus (ToLCNDV), a bipartite begomovirus prevalent in Old World and major cotton-growing regions of Pakistan, has increasingly been found associated with diverse betasatellites. Although betasatellites, small circular DNA satellites, are typically associated with monopartite begomoviruses, they are known to enhance disease severity (pathogenicity), increase viral DNA accumulation, and expand virus host ranges. This study investigated the interaction between ToLCNDV and three widely distributed betasatellites – cotton leaf curl Multan betasatellite strain Multan (Mβ), cotton leaf curl Multan betasatellite strain Burewala (Bβ) and tobacco leaf curl betasatellite (Tbβ) – in *Nicotiana benthamiana* plants, focusing on the potential emergence of novel viral combinations in cotton-growing regions. Infectious clones of ToLCNDV (either DNA-A [TA] alone or with DNA-B [TB]) were co-inoculated with each betasatellite clone. Results revealed intriguing complexity and variability in interactions: betasatellite with TA/TB affected TB accumulation, suggesting a competition between them, while TA levels increased only in the presence of TB, not apparently with Bβ. Interestingly, Tβ accumulated to the higher levels in plants, followed by Bβ and Mβ, highlighting betasatellite-specific interactions. These findings suggest that ToLCNDV-betasatellite interactions are more intricate than simple antagonism. The co-occurence of ToLCNDV with diverse betasatellites in cotton-growing regions of Pakistan increases the likelihood of the emergence of novel and potentially more pathogenic viral combinations. These intricate interactions have significant implications for understanding the dynamics of CLCuD disease.

OPEN ACCESS

Citation: Iqbal Z, Shafiq M, Ali S, Awan MF, Sarwar MF, Amin I, et al. (2025) Differential interactions of ToLCNDV with different betasatellites reveal complex viral dynamics in N. benthamiana. PLoS One 20(6): e0327234. https://doi.org/10.1371/journal.pone.0327234

Editor: Rajarshi Gaur, Deen Dayal Upadhyaya Gorakhpur University, INDIA

Received: January 13, 2025

Accepted: June 11, 2025

Published: June 25, 2025

Peer Review History: PLOS recognizes the benefits of transparency in the peer review process; therefore, we enable the publication of all of the content of peer review and author responses alongside final, published articles. The editorial history of this article is available here: https://doi.org/10.1371/journal.pone.0327234

Copyright: © 2025 Iqbal et al. This is an open access article distributed under the terms of the Creative Commons Attribution License, which permits unrestricted use, distribution,

and reproduction in any medium, provided the original author and source are credited.

Data availability statement: All the data related to this work is available in the manuscript and supplementary data. The research presented in this paper was originally conducted for the Ph.D. thesis of MS. This content has not been published elsewhere but a part of Higher education Commission (HEC) Pakistan's database.

Funding: The publication of this work was supported by the Deanship of Scientific Research (DSR), Vice Presidency for Graduate Studies and Scientific Research, King Faisal University, Saudi Arabia (KFU252251). The funder has no role in study design, data collection and analysis, decision to publish, or preparation of the manuscript.

Competing interests: The authors have declared that no competing interests exist.

1. Introduction

Tomato leaf curl New Delhi virus (ToLCNDV) is a highly widespread, prevalent and damaging bipartite begomovirus (family *Geminiviridae*), posing a significant threat to tomato production across three continents, including Asia, Africa, and Europe. It is a major impediment to agricultural productivity, particularly tomatoes, in South and Southeast Asia [1–3]. In recent years, it has expanded its reach from Asia to the Mediterranean region, causing concern in North Africa [4] and Southern Europe [5–7]. ToLCNDV infection leads to stunted growth and severe leaf curling in tomato plants and most plants it infects. ToLCNDV is a whitefly (*Bemisia tabaci*) transmitted bipartite begomovirus with two genomic components, DNA-A (TA) and DNA-B (TB), encoding eight genes. These genes are transcribed in both directions, virion-sense and complementary-sense, on both components. TA harbors genes for the coat protein (CP), pre-coat protein (AV2), and replication-associated protein (Rep), transcriptional activation (TrAP), replication enhancement (REn), and AC4. While TB encodes two proteins, the nuclear shuttle protein (NSP) and movement protein (MP), responsible for *in planta* movement. Prior studies have comprehensively characterized the functions of these genes and their crucial role in enabling successful infection by geminiviruses [8,9].

Most tomato infecting, single-stranded DNA begomoviruses from the Old World (OW) have monopartite genome and are associated with betasatellites. These small, circular, and single-stranded DNA molecules (genus *Betasatellite*, family *Tolecusatellitidae*) depend on their helper virus for replication, encapsidation, transmission, and *in planta* movement, and are in many cases, symptom determining [10–13]. Since their discovery in 1999, over 1300 isolates have been identified from 37 countries. Betasatellites typically harbor a single functional gene (βC1) on complementary-sense strand, which performs all the functions of betasatellite. There are, however, some exceptions, where another gene, referred to as βV1, is encoded on virion-sense strand and plays a critical role in infection, inducing mosaic and chlorosis symptoms [14]. Additionally, βV1 can elicit hypersensitive response (HR)-type cell death associated with reactive oxygen species (ROS) accumulation. Furthermore, βV1 can interact with the REn of helper virus [15]. On the other hand, βC1 performs diverse functions, including regulation of host microRNA levels [16], suppression of host defense at transcriptional gene silencing (TGS) and post transcriptional gene silencing (PTGS) [17,18], disrupt structure and functions of chloroplast [19], binds to DNA and RNA [20], subvert antiviral defense by interacting with extrinsic protein of Photosystem II (PsbP) and SNF1-related protein kinase (snRK1) [21,22], prevent degradation of viral protein by inhibiting the ubiquitin conjugase E2 which is involved in proteasome pathway [23], exhibits ATP hydrolysis activity that influences its DNA-binding activity and viral pathogenesis [24], and even suppresses the plant's jasmonic acid production [25].

Though bipartite begomoviruses are typically not associated with betasatellites, rare exception exists, including mung bean yellow mosaic India virus [26–28] and tomato yellow leaf curl Thailand virus [29]. Nonetheless, ToLCNDV has frequently been found associated with different betasatellites under natural conditions in

Pakistan and India. It has been found associated with cotton leaf curl Multan betasatellite strain Multan (Mβ), cotton leaf curl Multan betasatellite strain Burewala (Bβ) [30,31], chilli leaf curl betasatellite [32,33], tomato yellow leaf curl Thailand betasatellite [34], papaya leaf curl betasatellite [35], tomato leaf curl Jodeybpur betasatellite [36], tobacco leaf curl betasatellite (Tbβ) [37], and tomato leaf curl Bangladesh betasatellite [38] (S1 Table in S1 File). Additionally, ToLCNDV has been shown to trans-replicate different betasatellites in *N. benthamiana* plants under experimental conditions, including Mβ [39,40], tomato yellow leaf curl Thailand betasatellite, tomato leaf curl Patna betasatellite, radish leaf curl betasatellite, and tomato leaf curl Joydebpur betasatellite [41], and tomato leaf curl Bangladesh betasatellite [42].

Cotton leaf curl disease (CLCuD), a devastating disease caused by begomoviruses and their associated betasatellites, first emerged in Punjab in the 1960s [43]. After a period of localized outbreaks, a severe epidemic swept through Punjab in the 1990s, causing substantial economic losses reaching up to US$ 5 billion [44]. The emergence of resistant cotton varieties initially curbed the disease, but this resistance was short-lived, leading to a second epidemic in the early 2000s [45]. The first epidemic was primarily associated with Cotton leaf curl Multan virus (CLCuMuV) and Cotton leaf curl Kokhran virus (CLCuKoV), while the second was dominated by a recombinant CLCuKoV strain (CLCuKoV-Bur) [46]. In Sindh and northwestern India, greater begomovirus diversity persists, with CLCuKoV-Bur co-existing with other virus species. Recent reports indicate a resurgence of begomoviruses associated with the first epidemic of CLCuD in Pakistan [47] and India [48]. Additionally, ToLCNDV has also been reported in CLCuD-infected cotton in Pakistan [49]. A recent study [50] reported the presence of a novel and distinct CLCuMB lineage in Northwest India, alongside three alphasatellite species associated with CLCuD. This discovery underscores the ongoing evolution and diversification of the CLCuD disease complex in the region, particularly in the context of the widespread presence of ToLCNDV, which may further contribute to the emergence of novel and potentially more virulent viral combination.

Previous research using gene mutations in cotton leaf curl Kokhran virus and ToLCNDV [39,51] revealed the intricate interplay between betasatellites and gene mutants of their helper viruses, extending beyond just trans-replication and movement. While interaction between monopartite begomoviruses and their associated betasatellites have been extensively studied, knowledge about their interaction with bipartite begomoviruses remained an enigma. This complex interaction between ToLCNDV and betasatellites significantly worsens disease severity, yield losses, and economic hardship for farmers [38]. As these three betasatellites are frequently found associated with cotton infecting begomoviruses where ToLCNDV is also present, so there is a high potential for interaction that could lead to the emergence of a new viral combination with severe negative impact on crops. Therefore, understanding this intricate relationship is crucial for developing effective control strategies. This study aimed to investigate the interaction between ToLCNDV and diverse betasatellites.

2. Materials and methods

2.1. Origins of ToLCNDV and betasatellite clones and primers used in the study

Infectious binary vector constructs of TA (GenBank accession number U15015), TB (GenBank accession number U15016) [1], Mβ (GenBank accession number AJ292769) [13], Bβ (GenBank accession number AM774307) [46], and Tbβ (GenBank accession number AM922485) [26] have been described earlier. These constructs were electroporated into Agrobacterium tumefaciens (GV-3101) for inoculation in Nicotiana benthamiana plants.

To design primers for real time PCR and southern blot probe, sequences of TA, TB, Mβ, Bβ and Tbβ were retrieved from NCBI GenBank (https://www.ncbi.nlm.nih.gov/; accessed on December 2015). Each set of retrieved sequences were aligned in MEGA using Clustal X2 [52]. Then different set of oligonucleotide primers were designed on the highly conserved regions identified in a multiple sequence aligned files (S2 Table; S1 Fig in S1 File).

2.2. Sequence alignment and SCR analysis

The nucleotide sequences of all three betasatellites were retrieved from NCBI (https://www.ncbi.nlm.nih.gov/) and aligned using MEGA11 for multiple sequence comparison. Two datasets were then generated: one containing the coding

sequence (CDS) of βC1 and the other representing the satellite conserved region (SCR) and some of its upstream region. The βC1 sequences were translated into amino acids to evaluate their similarity at the protein level. Additionally, we conducted conserved repetitive motif analysis within the SCR of the three betasatellites using NovoPro's repeat sequence finder (https://www.novoprolabs.com/tools/repeats-sequences-finder) to identify shared regulatory elements.

2.3. Agroinoculation of *N. benthamiana* plants

A. tumefaciens (GV3101) cultures were grown in LB medium supplemented with rifampicin (25 μg.mL^{-1}), kanamycin (50 μg.mL^{-1}), and tetracycline (50 μg.mL^{-1}) at 28 °C for 48 h to an OD600 of 0.6–0.8. After centrifugation (5,000 × g for 15 min at 20°C), cells were resuspended in 10 mM $MgCl_2$ solution, adjusted to a uniform OD of 2.0. The Agrobacterium inoculums were further diluted to an OD of 1.0 and different inoculums were mixed to ensure that all plants receive equal concentration (OD = 0.3) of each construct. Finally, the inoculum was incubated for 1 h at room temperature containing 150 μg.mL^{-1} acetosyringone. A. tumefaciens cultures harboring the infectious constructs were inoculated into N. benthamiana plants (6–8 leaf stage). A group of six control plants received mock inoculation with Agrobacterium inoculum containing only the binary vector without the construct. Two to three leaves per plant were infiltrated with 0.5–1 mL of inoculum using a sterile 1 mL syringe [53]. For each experiment, control (healthy) plants without Agroinfiltration were included and each treatment involved inoculating six plants, with the experiment being repeated three times. The plants were housed in a pest-free glasshouse and monitored closely for symptom development each day. At 25 days post-inoculation (dpi), young leaf samples (emerging after inoculation) were used for DNA extraction and subsequent analysis using quantitative real-time PCR (qPCR) and Southern blotting. Plants were photographed prior to the sample collection.

2.4. Southern blot hybridization and bands quantification

Genomic DNA was extracted from 100 mg of leaf tissue using the CTAB method [54]. This DNA, isolated from two individual plants confirmed positive for viral components by PCR, was then analyzed by Southern blotting. For each sample, 8 μg of DNA was electrophoresed on agarose gels (1.5%), transferred to nitrocellulose membranes, and hybridized with α32P-dCTP labelled probes, following standard protocols [55]. Specific probes were used for the detection of TA (628 bp fragment of the Rep Gene), TB (475 bp fragment of the MP gene), and respective βC1 gene of each betasatellites (S1 Table; S1 Fig in S1 File). Following hybridization, detection was performed using a phosphor screen scanned on a Pharos FxTM system and analyzed with Quantity one software (version 4.6.9). Southern blots were performed on experiment 3 plants.

Southern blot band intensities were quantified using ImageJ software [56]. For each blot, the positive control band (TA in TA-inoculated plants, TB in TA/TB-inoculated plants, and betasatellite in TA/betasatellite-inoculated plants) was set to 100%, and all other bands were quantified relative to this control.

2.5. Quantitative analysis of the viral components

Genomic DNA from each plant was subjected to qPCR using the Chromo4TM PCR Detection System (Bio-Rad). The SYBR Green PCR Master Mix (ThermoFisher Scientific, Germany) was used for the assay, with specific primers designed (S1 Table in S1 File) to quantify each target viral component. Both reaction mixture and PCR conditions have already been described [57,58]. Standard curves were generated using ten-fold serial dilutions of standards (plasmid DNA spiked with N. benthamiana DNA) and melt curve analysis (S2 Fig in S1 File) was performed as outlined earlier [57]. The expression of each studied component was normalized to the 18S RNA housekeeping gene. Extracted DNA from the leaves of healthy N. benthamiana and mock inoculated plants were used as a negative control in qPCR assay. qPCR was performed on three biological replicates (comprising of three independent experiments), each with three technical replicates. Data from one representative biological replicate (Experiment 3) is presented for clarity and conciseness.

2.6. Standard curve analysis

Following each qPCR run, standard curve analysis was performed for TA, TB, and betasatellites amplicons using linear regression. This analysis plotted threshold cycles (Ct) values plotted against the input DNA amount. All the curves for each studied viral component demonstrated a linear relationship, and each sample showed a single peak, confirming the amplification of a single amplicon (S2 Fig in S1 File).

2.7. Molecular docking

To investigate the interaction between the Rep protein and target DNAs, molecular docking studies were performed. The three-dimensional (3D) structure of the Rep protein and DNA sequences representing the conserved region (CR) of TB, and the SCR of three betasatellites were constructed in silico. All molecular structures were prepared and saved in Protein Data Bank (.pdb) format using BIOVIA Discovery Studio Visualizer (v. 2024). Subsequently, protein-nucleic acid docking was carried out using the HDOCK server (http://hdock.phys.hust.edu.cn). The HDOCK server was selected for its specialized capability in performing protein-nucleic acid molecular docking analysis [59]. The respective .pdb files of the Rep protein and the DNA molecules were uploaded and processed through the server.

The resulting docked complex files, generated by the HDOCK server in.pdb format, were then analyzed using BIOVIA Discovery Studio Visualizer. Post-processing of these results included visualization of the docked structures, identification of interacting atoms, and figure generation.

2.8. Statistical analysis

The analysis of the qPCR data was performed using OriginPro software (version 10.1). Each treatment group consisted of three replicates ($n = 3$), and the mean values were employed for the analysis. One-way analysis of variance (ANOVA) was conducted to assess differences between multiple groups, followed by Tukey's post-hoc test for pairwise comparisons at $p \leq 0.05$.

3. Results

3.1. Sequence analysis of βC1 and SCR of the betasatellites

Pairwise sequence analysis of the βC1 protein region revealed that Tbβ exhibited a sequence identity of 15% and 15.8% with Bβ and Mβ, respectively, indicating a relatively distant evolutionary relationship. In contrast, Bβ and Mβ shared a significantly higher sequence identity of 96.1%, suggesting a closer evolutionary relationship between these two betasatellites (S3A Fig in S1 File).

Similarly, the SCR of Tbβ was more dissimilar to Bβ and Mβ compared to the similarity between Bβ and Mβ. While the SCR of Bβ and Mβ shared a significantly higher sequence identity, suggesting a conserved region important for their function or interaction with other viral components. (S3B Fig in S1 File). Analysis of the satellite conserved region (SCR) and its upstream region in TA, TB, and the three betasatellites revealed variations in conserved motifs and differing levels of similarity to TA. TB exhibited the greatest similarity to TA, sharing the first motif (5'-GGTGTCT-3') and differing only in the second (5'-GGCGTCT-3' vs. 5'-GGTGTCT-3' in TA). Bβ's first motif (5'-GGTGTTC-3') showed a slight variation, while its second (5'-GGTGTGT-3') diverged further. Tbβ's motifs (5'-GGCGTCA-3' and 5'-GGCGTAA-3') displayed moderate divergence from TA. Notably, Tbβ and Bβ shared a striking proximity in the location of their first motifs, hinting at a possible shared functional significance. Mβ was the most dissimilar, with both motifs (5'-GGTGATC-3') distinct from TA. These motif variations likely contribute to observed functional differences, including Bβ's superior performance over Mβ, despite 96.1% βC1 similarity.

3.2. Inoculation of ToLCNDV alone and with different betasatellites

N. benthamiana plants inoculated with only TA resulted in milder disease symptoms (100% infection) compared to those inoculated with both TA and TB (Fig 1A). These mild symptoms, characterized by upward leaf curling, emerged on newly developing leaves at 9 dpi and remained the same until the sampling time at 25 dpi.

In contrast, N. benthamiana inoculated with both TA and TB led to severe infection in all the inoculated plants. Notably, there was no difference in latent period and the first visible symptoms were upward leaf curling (Fig 1B; Table 1). Nonetheless over time, the severity of the symptoms intensified, leading to pronounced upward leaf curling.

Importantly, all non-inoculated control (healthy) plants and mock-inoculated plants remained symptomless throughout the experiment and were comparable to each other (Fig 1I, 1J).

The investigation into the co-infection effects of ToLCNDV and three associated betasatellites on N. benthamiana plants revealed a fascinating interplay between these pathogens. Co-inoculationof TA and TB along with Mβ resulted in a 100% infection rate in N. benthamiana plants, but with characteristic difference in symptoms. Interestingly, the primary symptom observed was a downward leaf curl, contrasting with the upward curling seen in TA/TB co-infection (Fig 1C). Notably, the symptoms onset was delayed, appearing at 10 dpi compared to 9 dpi observed with TA/TB (Table 1). This infection intensified over time, resulting in severe downward leaf curling and leaf crumpling.

Interestingly, co-inoculation of just TA along with Mβ also led to a 100% infection, but milder than TA/TB/Mβ inoculated plants (Fig 1D). Again, symptoms onset was slightly delayed (10 days compared to 9 days without the betasatellite; Table 1). The observed symptoms in this case were mild downward leaf curling of the edges of the leaves, forming inverted cup shape like structure with vein swelling (Fig 1D). This phenotype remained consistent throughout the experiment period.

In stark contrast to TA/Mβ inoculated plants, all the N. benthamiana plants inoculated with TA/Bβ or TA/TB/Bβ displayed symptoms more reminiscent of TA/TB than those observed with a betasatellite. These symptoms included upward leaf curling and vein swelling (Fig 1E,1F).

Notably, N. benthaimana plants co-inoculated with TA/TB and Tbβ exhibited a substantially distinct disease phenotype compared to those co-inoculated with either Mβ or Bβ. Unlike the characteristic upward curling and crumpling seen with the latter two, Tbβ co-inoculated plants exhibited a distinctive downward curling (invert cupping) of leaves (Fig 1G,1H). This cupping effect was accompanied by less crumpling and visible swelling of the veins. Interestingly, the latent period remained consistent at 10 days post-inoculation (dpi) regardless of Tbβ presence. However, a crucial difference emerged in the severity of the symptoms between plants infected with TA/TB alone and those TA/TB and Tbβ. In the absence of

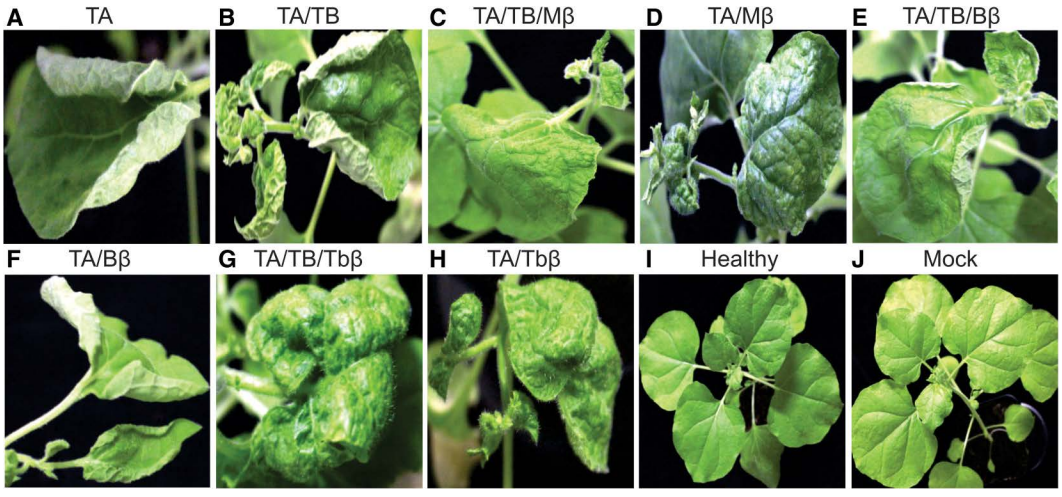

Fig 1. Impact of different betasatellites on symptom development in ToLCNDV-inoculated *N. benthamiana* plants. Plants were inoculated with TA (A), TA and TB (B), TA, TB and Mβ (C), TA and Mβ (D), TA, TB and Bβ (E), TA and Bβ (F), TA, TB and Tbβ (G), TA and Tbβ (H, non-inoculated (Healthy; I) and mock (J). Abbreviations used in the figure are ToLCNDV DNA-A (TA), DNA-B (TB), cotton leaf curl Multan betasatellite (Mβ), cotton leaf curl Multan betasatellite strain Burewala (Bβ), and tobacco leaf curl betasatellite (Tbβ).

https://doi.org/10.1371/journal.pone.0327234.g001

TB, the symptoms were a bit milder. Furthermore, the presence of Tbβ appeared to influence the progression of symptoms over time.

3.3. Southern blot detection and quantification of viral components

Southern blot band intensities were quantified for each viral component, ensuring that band signals remained within the linear range of detection and exhibited minimal background noise. Within each blot, the corresponding positive control band (TA in TA-inoculated plants, TB in TA/TB-inoculated plants, and betasatellite in TA/betasatellite-inoculated plants) was normalized to 1.0 (100%), and all other bands were quantified relative to this control, and results are depicted in ratios (S4 Fig in S1 File). Notably, TA DNA was consistently detected in all inoculated plants, regardless of whether they were co-infected with TB or with different betasatellites (Mβ, Bβ, or Tbβ). TA DNA levels were slightly higher in plants co-inoculated with TB (1.38) compared to plants inoculated with TA alone (1.0). This indicates that TA establishes itself within the plant system. However, co-inoculation with any of the betasatellite further elevated TA levels, suggesting that these satellite molecules may influence TA accumulation or persistence within the host plant (Fig 2). Among the different co-infections involving betasatellites, Tbβ co-inoculation resulted in the highest accumulation of TA DNA (2.08–2.43), followed by Mβ (1.46–1.64) and Bβ (1.39–1.57), respectively (S4A Fig in S1 File). This finding suggests that Tbβ might be particularly adept at enhancing TA replication or persistence within the host than Mβ and Bβ (Fig 2). TA ssDNA quantification showed the similar results with the highest levels in Tbβ co-inoculations, followed by Mβ, and the lowest in Bβ co-inoculations. This suggests varying influences of the betasatellites on TA replication, with Tbβ exhibiting the strongest synergistic interaction (S4B Fig in S1 File).

In Southern blot analysis, TB was successfully detected in plants inoculated with either TA/TB or in combination with any of the betasatellites (TA/TB/betasatellite) (Fig 3). The TB was accumulated to a highest level in TA/TB inoculated plants (1.0) than in presence of any betasatellite; TA/TB/Mβ (0.59), TA/TB/Bβ (0.74), and TA/TB/Tbβ (0.96) (S4C Fig in S1 File). Importantly, none of the control plants reveal the detection of either TA nor TB (Fig 3). This negative result in control plants strengthens the validity of the experiment and confirms the specificity of the probe used. It is noteworthy that the Southern blot for TB detection required an extended exposure time to the phosphor imager to yield the visible results.

Table 1. Evaluation of ToLCNDV infectivity in *N. benthamiana* plants co-inoculated with various betasatellites.

Inoculum	Infectivity						Symptoms[$]	Symptoms Severity Score	Latent period (days)
	Diagnostics by qPCR (plants infected/ inoculated)[*]			Southern					
				TA	TB	Beta			
				TA	TB	Beta			
TA	18/18	--	--	+	--	--	MULC	+	9
TA/TB	18/18	18/18	--	+	+	--	SULC,VT	++	9
TA/TB/Mβ	18/18	18/18	18/18	+	+	+	SDLC,VT	+++	10
TA/Mβ	18/18	--	18/18	+	--	+	MULC,VT	+++	10
TA/TB/Bβ	18/18	18/18	18/18	+	+	+	SULC,VT	++	10
TA/Bβ	18/18	--	18/18	+	--	+	MULC	+	10
TA/TB/Tbβ	18/18	18/18	18/18	+	+	+	SDLC,VT	+++	10
TA/Tbβ	18/18	--	18/18	+	--	+	SDLC,VT	+++	10

[*]Cumulative average of three independent experiments. Each experiment comprised 6 plants per inoculum type.

[$]Symptoms are denoted are mild upward leaf curling (MULC), severe upward leaf curling (SULC), severe downward leaf curling (SDLC), and vein thickening (VT). Two consecutive dash lines (--) represents viral component was not used in the inoculum. Abbreviations used in the table are ToLCNDV DNA-A (TA), DNA-B (TB), cotton leaf curl Multan betasatellite (Mβ), cotton leaf curl Multan betasatellite strain Burewala (Bβ), and tobacco leaf curl betasatellite (Tbβ).

https://doi.org/10.1371/journal.pone.0327234.t001

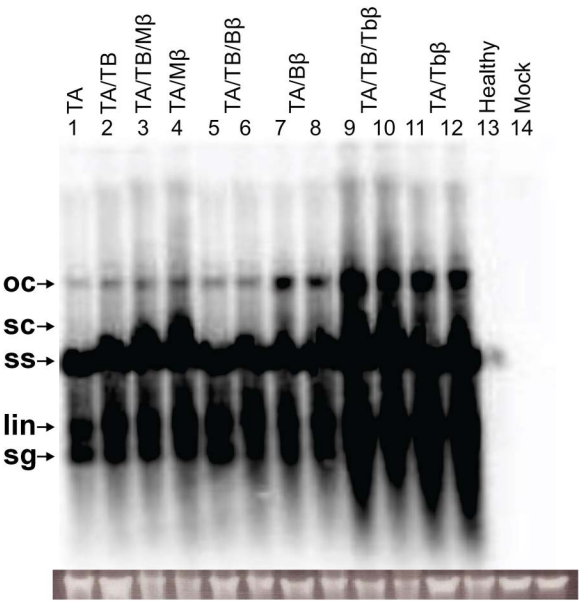

Fig 2. Southern blot for the detection of TA in agro-inoculated *N. benthamiana* plants. DNA samples from leaf extracts were run on agarose gel: TA (lane 1), TA and TB (lanes 2), TA, TB and Mβ (lanes 3), TA and Mβ (lanes 4), TA, TB and Bβ (lanes 5 and 6), TA and Bβ (lanes 7 and 8), TA, TB, and Tbβ (Lanes 9 and 10), TA and Tbβ (Lanes 11 and 12), non-inoculated healthy plant (lane 13) and a mock inoculated plant (lane 14). The agarose gel image (shown below the Southern blot) confirms equal loading of DNA samples. Viral DNA forms are labelled as linear (lin), open-circular (oc), single-stranded (ss), super-coiled (sc), and sub-genomics (sg). Abbreviations used in the figure are ToLCNDV DNA-A (TA), DNA-B (TB), cotton leaf curl Multan betasatellite (Mβ), cotton leaf curl Multan betasatellite strain Burewala (Bβ), and tobacco leaf curl betasatellite (Tbβ).

https://doi.org/10.1371/journal.pone.0327234.g002

Further Southern blot analysis focused on the detection of specific betasatellites. Mβ was detected in plants co-inoculated with either TA or TA/TB. Mβ accumulation, as indicated by band intensity and replicative forms, was slightly higher in TA/TB/Mβ-inoculated plants (0.83–1.0) compared to TA/Mβ-inoculated plants (0.71–0.79) (Fig 4A; S4D Fig in S1 File). This higher accumulation suggests that the presence of TB might enhance the Mβ accumulation. In stark contrast to Mβ, the Southern blot analysis of Bβ and Tbβ (Figs 4B and 4C, respectively) revealed slightly higher accumulation. Plants co-inoculated with TA/Bβ or TA/TB/Bβ displayed comparable levels of betasatellites, ranging from 1.0 to 1.15. Likewise, Tbβ inoculated plants showed higher accumulation of Tbβ (1 to 1.23) compared to the other two betasatellites. These observations suggested that presence or absence of TB did not significantly affect the accumulation levels of Bβ and Tbβ. Notably, DNA from plants inoculated with other betasatellites was included as controls in each gel. For instance, in the Mβ Southern blot, DNA from Bβ-inoculated plants was included. No cross-detection of betasatellites was observed, suggesting highly specific detection methods.

3.4. qPCR-mediated quantification of viral components

To ensure consistency in the results, we included data from plants analyzed using Southern blotting alongside other plants. Furthermore, qPCR assays incorporated multiple biological and technical replicates to enhance statistical robustness. Rigorous optimization of qPCR conditions, including primer concentrations and thermocycler settings, was performed to guarantee consistent and efficient amplification across all viral components. Melt curve analysis of the qPCR reactions revealed a single, distinct peak, confirming the amplification of a unique and specific product for each target. This observation indicates high specificity and the absence of non-specific amplification or primer-dimer formation. While significant variation in the levels of viral DNA components was observed across all plants, the mean and cumulative average of viral DNA and their associated betasatellites are mentioned in the folllwing results.

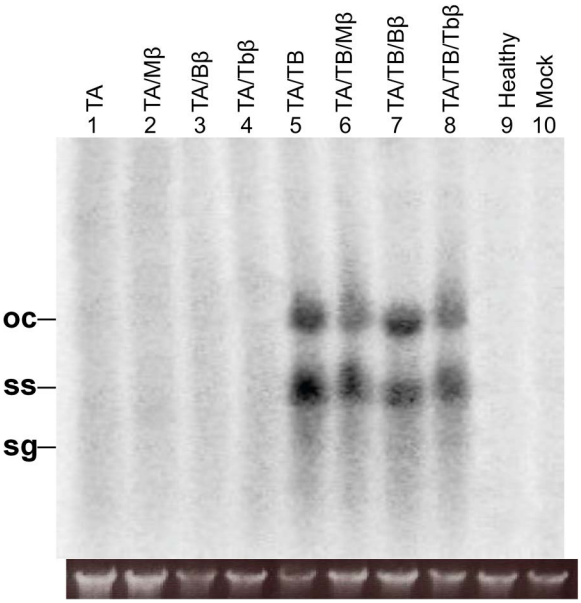

Fig 3. Southern blot for the detection of TB in agro-inoculated *N. benthamiana* plants. The DNA samples loaded onto the gel came from the leaves of plants that inoculated with TA (lanes 1), TA and Mβ (lane 2), TA and Bβ (lane 3), TA and Tbβ (lane 4), TA and TB (lane 5), TA, TB and Mβ (lane 6), TA, TB and Bβ (lane 7), and TA, TB and Tbβ (lane 8), and of control plants, healthy (non-inoculated) (lane 9) and a mock plant (lane 10). The agarose gel image (shown below the Southern blot) confirms equal loading of DNA samples. Abbreviations used in the figure are ToLCNDV DNA-A (TA), DNA-B (TB), cotton leaf curl Multan betasatellite (Mβ), cotton leaf curl Multan betasatellite strain Burewala (Bβ), and tobacco leaf curl betasatellite (Tbβ).

https://doi.org/10.1371/journal.pone.0327234.g003

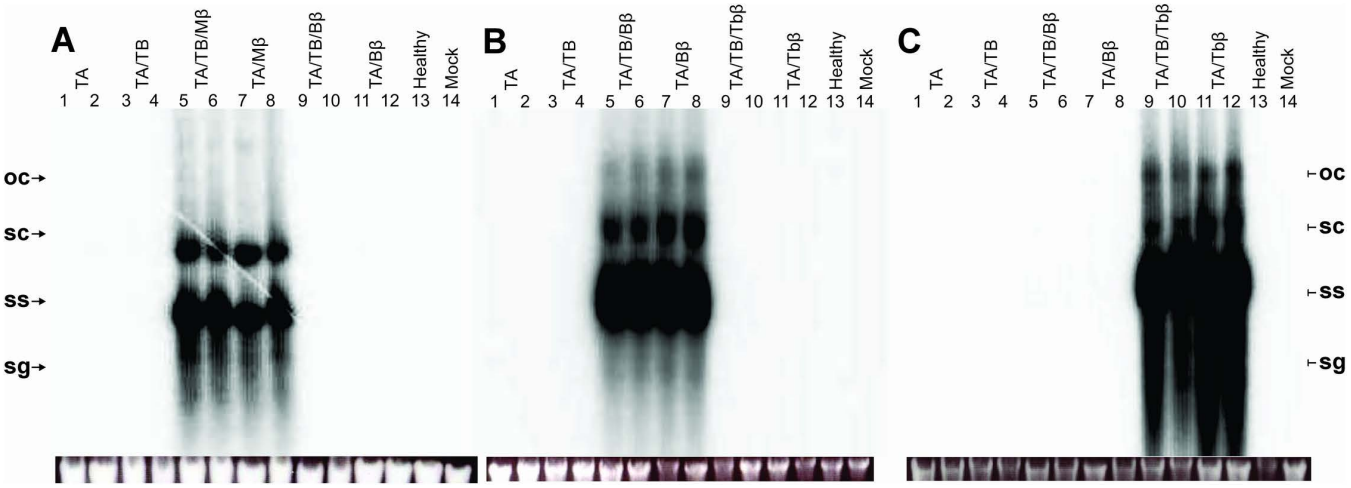

Fig 4. Southern blot Mβ (A), Bβ (B) and Tbβ (C) in agro-inoculated *N. benthamiana* plants. For the detection of Mβ (A), DNA samples extracted from leaves of plants inoculated with TA (lanes 1 and 2), TA and TB(3 and 4), TA, TB and Mβ (5 and 6), TA and Mβ (7 and 8),TA, TB and Bβ (9 and 10),TA and Bβ (11 and 12), healthy (non-inoculated) plant (13) and a mock inoculated plant (lane 14). The agarose gel images (shown below the Southern blot) confirm equal loading of DNA samples. Abbreviations used in the figure are ToLCNDV DNA-A (TA), DNA-B (TB), cotton leaf curl Multan betasatellite (Mβ), cotton leaf curl Multan betasatellite strain Burewala (Bβ), and tobacco leaf curl betasatellite (Tbβ).

https://doi.org/10.1371/journal.pone.0327234.g004

In qPCR analysis, none of the viral components were detected in control plants, validating the specificity of qPCR and experimental setup. The mean value of the measured titers of TA in plants inoculated with TA/TB were insignificantly higher (0.0955 ng/μg of genomic DNA) compared to TA inouclated plants (0.0645 ng/μg of genomic DNA) (Fig 5A). The presence or absence of betasatellites significantly affect TA titers in TA/TB co-inoculated plants. Interestingly,TA titers were nearly doubled in plants inoculated with TA/betasatellites compared to those inoculated with TA/TB/Mβ. Notably, the highest TA accumulation (0.457 ng) was observed in plants inoculated with TA/TB/Tbβ (Fig 5A).

The TB DNA was not detected in control plants, and those inoculated with TA, TA/Mβ, TA/Bβ, and TA/Tbβ, validating the qPCR results (Fig 5B). Interestingly, plants inoculated with TA/TB/betasatellite led to a slightly higher TB accumulation than TA/TB plants. In TA/TB/Mβ, TA/TB/Bβ, and TA/TB/Tbβ plants, TB titers were slightly high, reaching a mean value of 0.00049, 0.000495, and 0.00052 ng/μg of genomic DNA, respectively, compared to 0.00047 ng/μg of genomic DNA in plants inoculated with TA/TB (Fig 5B). While our data showed slightly elevated TB titers, it's important to note that this increase was not statistically significant.

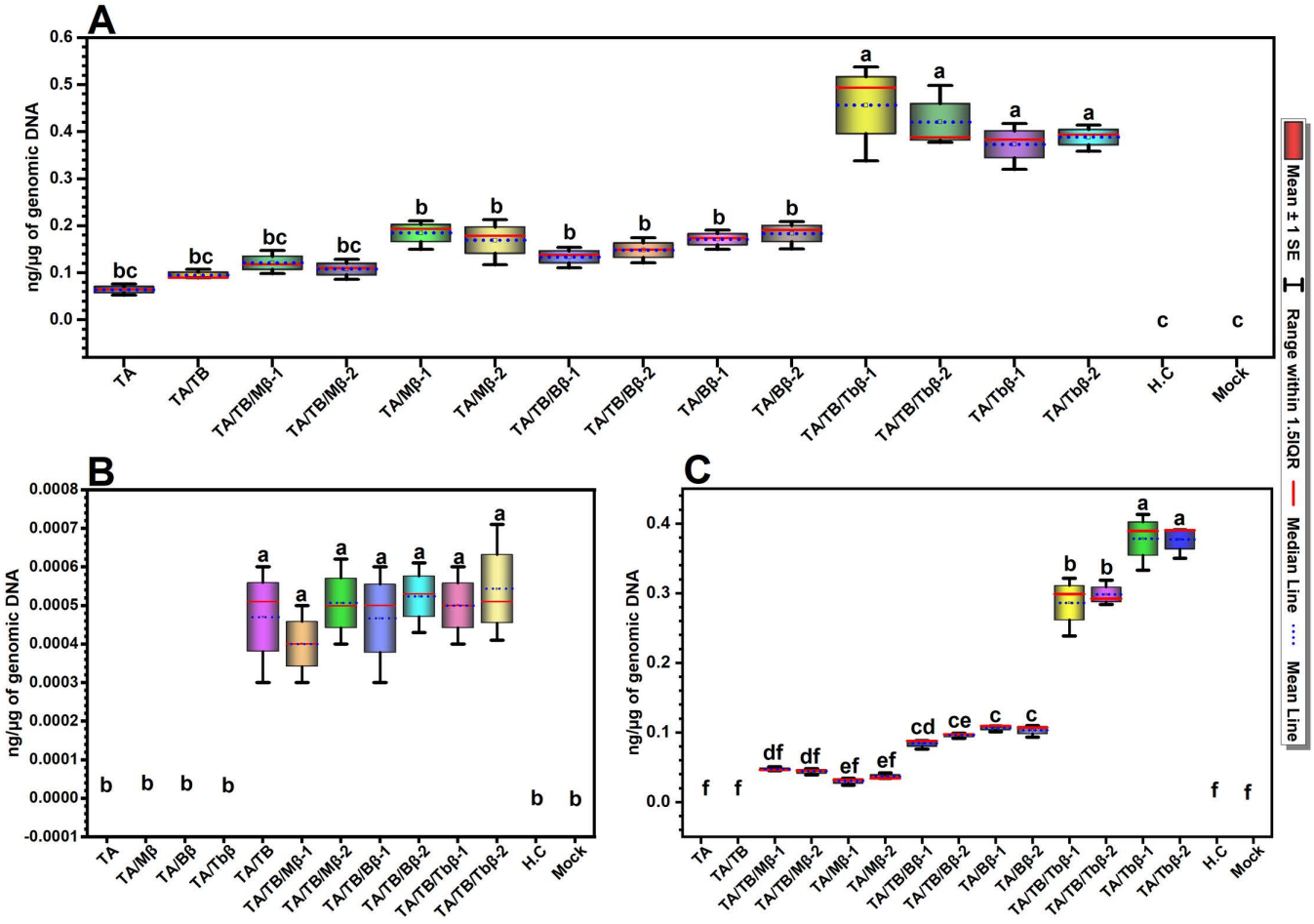

Fig 5. Estimation of the DNA titers of TA (A), TB (B) and betasatellite (C) in the inoculated plants, control healthy (non-inoculated; H.C) and mock plants. The experiment was repeated three times, with samples from each experiment analyzed in triplicate (technical repeats). The data presented in the figure represents the mean values obtained from three independent replicates (n = 3). Statistical analysis was performed, and groups denoted by different lowercase letters differ significantly from each other at a 5% significance level ($p \leq 0.05$). Abbreviations used in the figure are ToLCNDV DNA-A (TA), DNA-B (TB), cotton leaf curl Multan betasatellite (Mβ), cotton leaf curl Multan betasatellite strain Burewala (Bβ), and tobacco leaf curl betasatellite (Tbβ). Median and mean are shown in solid red and dotted blue lines, respectively.

https://doi.org/10.1371/journal.pone.0327234.g005

qPCR analysis revealed significant differences in betasatellite accumulation. Tbβ exhibited significantly higher titers than Mβ and Bβ in all combinations, reaching ~0.298 and 0.378 ng/μg of genomic DNA in TA/TB/Tbβ and TA/Tbβ plants, respectively. Mβ showed the lowest accumulation, with titers around 0.047 and 0.037 ng/μg of genomic DNA in TA/TB/Mβ and TA/Mβ plants, respectively. Bβ titers were significantly higher than Mβ, reaching 0.096 and 0.106 ng/μg of genomic DNA in TA/TB/Bβ and TA/Bβ plants, respectively (Fig 5C).

3.5. Molecular docking of rep with CR of TB and SCR of betasatellites

Molecular docking analysis revealed distinct binding affinities and interaction energies between the Rep protein and each DNA sequence (S3 Table in S1 File). The Rep-TA (−241.17 kJ.mol^{-1}) and Rep-Tbβ (−189.72 kJ.mol^{-1}) complexes exhibited the highest binding affinity (lowest binding energies), followed by Rep-TB (−184.60 kJ.mol^{-1}), Rep-Bβ (−184.11 kJ.mol^{-1}), and Rep-Mβ (−184.09 kJ.mol^{-1}), suggesting a hierarchy in Rep's binding preference. In addition, this trend was further supported by the intermolecular interactions, which consistently followed the same affinity ranking.

In a competitive biological context—where Rep mediates the replication of multiple viral components—these findings imply that Rep likely prioritizes binding to TA, Tbβ, and TB due to its stronger affinity, potentially outcompeting with other betasatellites with weaker interactions. Notably, while Bβ and Mβ shared the same binding site and energy on Rep, Bβ formed more stabilizing interactions and close proximity (S5 Fig in S1 File), which may explain its comparatively better maintenance over Mβ in viral replication.

4. Discussion

Bipartite begomoviruses are increasingly being detected in the field alongside betasatellites, underscoring the need of investigation [31,60,61]. Among the bipartite begomoviruses, ToLCNDV stands out for its exceptionally broad host range and frequent association with diverse betasatellites, making it an intriguing subject for investigation. Furthermore, its widespread presence in cotton-growing areas, coupled with the rapid spread of PeLCV (along with its cognate betasatellite, TbLCB), raises concerns about the potential emergence of novel and more virulent viral combinations. This epidemiological context underscores the need to investigate the potential interactions between ToLCNDV and these diverse betasatellites (CLCuMB, CLCuMB-Bu, and TbLCB) to assess their impact on disease severity. While interactions and effects of betasatellites with monopartite begomoviruses have been extensively studied [40,51,62,63], the impact of their association with bipartite counterparts remains largely unexplored. This study aims to fill this gap by investigating the interaction of betasatellites with a bipartite begomovirus.

While bipartite begomoviruses typically require both DNA-A and DNA-B for symptomatic infection in plants, DNA-A (TA) alone has been shown to infect *N. benthamiana*, albeit inconsistently, with reduced viral titters and diminished infection efficiency [13,39,64,65]. Also, such infections seem limited to *N. benthamiana* and a typically observed only after Agro-inoculation, not mechanical or biolistic inoculation methods [1]. Our findings align with previous reports, with the exception of TA alone exhibiting symptoms albeit with milder symptoms, similar peculiar phenomena also observed by Jyothsna et al. [31]. Conversely, two other studies [39,66] observe asymptomatic infections with TA alone, suggesting isolate specific variations. Intriguingly, TA's systemic movement without TB deviates from typical bipartite begomovirus transport. This could reflect an evolutionary adaptation, perhaps analogous to monopartite begomoviruses, where TA may have acquired DNA-B while retaining independent movement, providing a selective advantage. Alternatively, its autonomous movement might be context-dependent, possibly only related to *N. benthamiana*'s lack of RDR6, a key player in antiviral silencing [67]. The absence of RDR6 could enable TA to bypass typical constraints. This unique behavior also raises the possibility of TA forming new pathogenic combinations by associating with other monopartite begomoviruses, the DNA B of bipartite begomoviruses, or satellites, potentially creating recombinant strains with altered disease dynamics, pathogenicity, and host range [68]. Understanding these mechanisms provides insights into the evolutionary flexibility of pathogen transport, aiding the development of innovative antiviral strategies and improving management of viral infections in key crops.

While co-inoculation with cognate betasatellites typically boosts monopartite begomovirus DNA titers [13,63,69,70], this study observed an intriguing exception. All the betasatellites increased TA titer but it was highest in the presence of Tbβ (Fig 5A). This suggests a positive influence of betasatellites on TA [31]. As we found here, they [31] observed that TB presence reduced betasatellite titer while the betasatellite presence enhanced TB titer. Notably, our study found that plants infected with Tbβ and Bβ showed significantly higher TB titers compared to those infected with TA and TB. The precise reason for this apparent antagonism is far from a conclusion. Our molecular docking results provided potential mechanistic insights, showing Rep's preferential binding to Tbβ and TB over other betasatellites, which might explain higher TB's replication advantage. This binding hierarchy could reflect competition for virus TA-encoded Rep by both DNA-B and betasatellites for replication, or interference with movement functions. As TB encoded proteins [71,72] and the βC1 protein [73] have movement functions, suggests a potential redundancy in the viral movement mechanism. This redundancy could potentially lead to competition or interference between the two mechanisms. Further research is needed to elucidate the molecular basis of the apparent antagonism. Or we may speculate that the difference likely stems from variations in viral isolates/strains, experimental conditions/design, environmental conditions, and replication dynamics. Moreover, Mβ impaired ToLCNDV ability to maintain cotton leaf curl Multan alphasatellite in *N. benthamiana* plants [40], highlighting further complexities in the intricate interplay among begomovirus-betasatellite-alphasatellite.

Intriguingly, Tbβ induced more pronounced disease symptoms compared to Bβ and Mβ, with a significantly higher DNA titer (Fig 5), aligning with the earlier study showing higher betasatellite DNA levels enhanced symptoms severity, impaired plant performance, and lower seed yield [58]. This also imply that, beyond simple titre, Tbβ's specific interaction mechanisms with the host and ToLCNDV played a crucial role, underscoring the concept of betasatellite-specific interactions. The lower titers of Bβ and Mβ, despite their persistent association with CLCuD, are surprising. This disparity suggests that different betasatellites might employ distinct mechanisms to exploit the host environment and their cognate virus. For example, host factors can influence tissue-specific viral gene expression via interactions with viral gene promoter regions [74]. So, *N. benthamiana* environment appears to favor Tbβ's replication and its interaction with ToLCNDV, possibly due to elements like the G-box motif in the βC1 region of Tbβ, known to enhance betasatellite replication through interactions with host factors [75]. Furthermore, non-coding regions of satellite DNA, as identified by Li et al. [76] and Reddy et al. [77], are also critical for replication and symptoms induction. Further investigation of these non-coding regions in these complex interactions is warranted and could be the interest of futuristic studies. Our findings revealed unique interactions between ToLCNDV and even quite closely related betasatellites. While the underlying mechanisms require further study, several observations are noteworthy. First, TBβ, despite its soybean origin [26], impacted TA infections more strongly than either of the Mβ and Bβ, suggesting adaptation to *Solanaceous* plants. Second, the contrasting effects of the two CLCuMBs are surprising. Their key difference lies in a non-coding region of SCR encompassing approximately 110 nt fragment from tomato leaf curl betasatellite [78,79]. However, this difference is unlikely the primary driver of observed plant responses. Instead, the six amino acid differences within the βC1 protein of these clones are far more likely to be responsible [80], as all known betasatellite functions are attributed to the βC1 protein [63,81]. Furthermore, high-affinity interactions between Rep-binding sites in the betasatellite and Rep proteins may influence betasatellite titer levels [24,82]. Third, our docking analysis revealed a binding affinity hierarchy (Tbβ > Bβ > Mβ) mediated by differential bonding, suggesting Rep-binding site affinity influences betasatellite accumulation.

The intricate relationship between a bipartite begomovirus and its associated betasatellite extends far beyond a simple exchange of replication machinery. While likely targeting the same host cells for synchronized infection, betasatellite act as a master manipulator. It hijacks the begomovirus's replication machinery, diverting resources for its own replication and suppressing the host defense mechanisms, including TGS and PTGS [17]. Additionally, betasatellites may disrupt chloroplast function, which is crucial for autophagy-mediated degradation of viral proteins [19]. Some non-coding regions of satellite DNA are highly critical for the replication [76], and betasatellite lacking SCR (1190–1320 nt) and its downstream sequences (1091–1190 nt) are essential for replication and symptoms induction [77]. This strategic commandeering

enhances betasatellite amplification and viral movement [83]. Additionally, betasatellites contain iteron-like repeat motif (5'-GAGGACC-3' with 5'-GGACC-3' core), homologous to those in their cognate helper begomoviruses, which are essential for specific Rep binding [82]. Our SCR analyses revealed varying degrees of similarity in conserved repeat motifs across the studied betasatellites. Bβ's motifs exhibited the highest similarity to those in TA, followed by Tbβ. Mβ's motifs showed the least similarity. Notably, Tbβ and Bβ shared a striking proximity in the location of their first motifs, hinting at a possible shared functional significance. These results likely explain the observed performance variations, with Bβ outperforming Mβ despite 96.1% βC1 sequence similarity. This suggests Bβ's motifs are better recognized by Rep than those of Mβ. Collectively, this intricate interplay leads to disease severity, maintenance and trans-replication of betasatellites [31,84].

The stability of the tripartite begomovirus complex under natural *B. tabaci* transmission warrants serial passage experiments. Current field evidence, however, hints at potential stability, as demonstrated by the detection of ToLCNDV with Mβ in field-grown tomato and cotton [31,49]. Our findings further bolster this notion, demonstrating that ToLCNDV can maintain these three betasatellites (Tbβ, Bβ, Mβ), likely facilitated by the *B. tabaci*'s polyphagous nature and capacity to transmit multiple begomovirus components. Nevertheless, without longitudinal co-infection studies spanning multiple plant generations, this claim remains speculative. We acknowledge this as a limitation and propose future serial passage experiments to definitively assess the temporal stability of these associations, enhancing the robustness of our conclusions. It is highly likely that the intensifying agricultural practices in southern Asia will increase the encounter rate between bipartite begomoviruses and betasatellites during co-infections. However, predicting the outcome of these encounters remains elusive, as evidenced by current study and previous research. However, understanding the long-term impact of such interactions will be intriguing. Although betasatellites enhance pathogenicity, host adaptation, suppress RNA silencing, disrupt hormone signaling, causing severe symptoms and expanding the host range. But this dependence on betasatellites may pose evolutionary disadvantages, such as reduced adaptability in their absence, decreased host availability due to increased virulence, and stronger host resistance mechanisms. While betasatellites provide short-term advantages, they may impose long-term trade-offs for ToLCNDV.

While ToLCNDV remains the predominant begomovirus in the region, another bipartite begomovirus, tomato leaf curl Palampur virus (ToLCPalV), also circulates, albeit with a notably less distribution. ToLCPalV is found associated with Pepper leaf curl betasatellite and Mβ [85–87], yet its specific interactions and functional consequences of these associations remain unexplored. This lack of research presents a significant knowledge gap in understanding bipartite begomovirus dynamics. Unlike ToLCNDV, which exhibits widespread adaptability, ToLCPalV's limited range raises intriguing questions about the ecological and molecular factors—such as host specificity, vector efficiency, or Rep-mediated replication dynamics—driving their differential spread and adaptation. Future studies investigating the interactions between ToLCPalV and its associated betasatellites would be valuable in understanding the broader ecological and evolutionary dynamics of begomoviruses in this region. Co-infecting plants with bipartite begomoviruses and betasatellites, potentially through whitefly transmission, and monitoring their persistence over time could address critical questions about their survival dynamics and evolutionary advantages or disadvantages. These queries include: will the betasatellite or the DNA-B ultimately be lost, or could a stable tripartite association evolve? Answering these questions is paramount, as betasatellites are known to exacerbate disease symptoms (and thus losses) and broaden the host range of begomoviruses [26]. Unraveling the answers to these queries can pave way for effective strategies to mitigate the potential risks posed by betasatellite spread and their interaction with bipartite begomoviruses in this rapidly evolving agricultural landscape.

5. Conclusions

The interaction between a bipartite begomovirus and a betasatellite was found to be more intricate than just trans-replication of the satellite. Even closely related betasatellites exhibited diverse behaviors, highlighting the complexity of begomovirus-betasatellites interactions. While the apparent antagonism between the betasatellite and DNA-B suggests

a nuanced and potentially unstable relationship, it may not necessarily lead to the formation of super virulent tripartite viruses. However, the regular occurrence of these co-infections in the field underscores their potential to cause substantial economic losses in important crops.

Supporting information

S1 File. **S1 Table.** List of betasatellites found associated with ToLCNDV in Solanaceous crops. **S2 Table.** Oligonucleotide primers used in the study for quantification and Southern blotting. **S3 Table.** Rep-DNA docked complexes and their binding free energy. **S1 Fig.** Diagram showing the positions of primers on ToLCNDV DNA A (A), DNA B (B) and TbLCB (C) that were used in the quantitative PCR assays. **S2 Fig.** Standard curve and melt curve for amplification of ToLCNDV DNA A. (A) Standard curve for estimation of the titre of ToLCNDV DNA A with a PCR efficiency of 96.5%, slope of −3.376 and correlation coefficient 0.992 [left] and a melt curve analysis of the products of amplification [right]. (B) Standard curve for estimation of the titre of ToLCNDV DNA B with a PCR efficiency of 95.0%, slope of −3.376 and correlation coefficient 0.991 [left] and a melt curve analysis of the products of amplification [right]. (C) Standard curve for estimation of the titre of betasatellites with a PCR efficiency of 97.0%, slope of −3.376 and correlation coefficient 0.995 [left] and a melt curve analysis of the products of amplification [right]. The standard curves plot log of starting DNA quantity against threshold cycle [C(T)] cycle. The melt curves plots negative rate of change of fluorescence [-d(RFU)/dT] against temperature. **S3 Fig.** Alignment of coding region βC1 (A) and the satellite conserved region (SCR) (B) from three betasatellites: tobacco leaf curl betasatellite (Tbβ), cotton leaf curl Multan betasatellite (Mβ), and cotton leaf curl Multan betasatellite strain Burewala (Bβ). Sequence similarity is indicated by color: red for highly similar regions across all three betasatellites, green for regions similar in two betasatellites, and blue for dissimilar sequences. Identified repetitive motifs are enclosed in boxes: green for motifs common to all three betasatellites, brown for motifs shared by Tbβ and Bβ, and blue for motifs shared by Bβ and Mβ. Yellow boxes denote previously reported repetitive sequence motifs (Xu et al., 2019). Nonanucleotide sequences are highlighted in red boxes. **S4 Fig.** Quantification of Southern blot bands. Relative band intensities (quantification) from Southern blots are shown for ToLCNDV DNA A (A), single-stranded bands of ToLCNDV DNA A (B), ToLCNDV DNA B (C), and three different betasatellites (D). Band intensities were normalized to the corresponding positive control band within each blot, which was set to a value of 1. Panel (D) illustrates the accumulation of three betasatellites: Mβ (yellow), Bβ (blue), and Tbβ (cyan). **S5 Fig.** Molecular docking models illustrating the predicted binding interactions between the Rep protein and different DNA molecules: (A) Rep protein docked with CR of DNA-A; (B) Rep protein docked with CR of DNA-B; (C) Rep protein docked with SCR of Bβ; (D) Rep protein docked with SCR of Mβ; (E) Rep protein docked with SCR of Tbβ. Docked complexes are shown as representative structures from the HDOCK server, used for protein-nucleic acid docking analysis.
(DOCX)

S2 File.
(DOCX)

Acknowledgments

Authors acknowledge all the support staff in the lab for their assistance during this work.

Author contributions

Conceptualization: Zafar Iqbal, Muhammad Shafiq, Rob W. Briddon.

Formal analysis: Zafar Iqbal, Muhammad Shafiq, Sajed Ali, Mudassar Fareed Awan, Muhammad Farhan Sarwar.

Funding acquisition: Zafar Iqbal.

Investigation: Mudassar Fareed Awan.

Methodology: Zafar Iqbal, Muhammad Shafiq.

Project administration: Rob W. Briddon.

Supervision: Rob W. Briddon.

Validation: Zafar Iqbal.

Writing – original draft: Zafar Iqbal, Muhammad Shafiq, Imran Amin, Muhammad Shafiq Shahid, Rob W. Briddon.

Writing – review & editing: Zafar Iqbal, Imran Amin, Rob W. Briddon.

References

1. Padidam M, Beachy RN, Fauquet CM. Tomato leaf curl geminivirus from India has a bipartite genome and coat protein is not essential for infectivity. J Gen Virol. 1995;76(Pt 1):25–35. https://doi.org/10.1099/0022-1317-76-1-25 PMID: 7844539
2. Sahu PP, Rai NK, Chakraborty S, Singh M, Chandrappa PH, Ramesh B, et al. Tomato cultivar tolerant to Tomato leaf curl New Delhi virus infection induces virus-specific short interfering RNA accumulation and defence-associated host gene expression. Mol Plant Pathol. 2010;11(4):531–44. https://doi.org/10.1111/j.1364-3703.2010.00630.x PMID: 20618710
3. Mizutani T, Daryono BS, Ikegami M, Natsuaki KT. First report of tomato leaf curl New Delhi virus infecting cucumber in Central Java, Indonesia. Plant Dis. 2011;95(11):1485. https://doi.org/10.1094/PDIS-03-11-0196 PMID: 30731770
4. Mnari-Hattab M, Zammouri S, Belkadhi MS, Doña DB, Nahia E ben, Hajlaoui MR. First report of tomato leaf curl New Delhi virus infecting cucurbits in Tunisia. New Dis Rep. 2015;31(1):21–21. https://doi.org/10.5197/j.2044-0588.2015.031.021
5. Juárez M, Tovar R, Fiallo-Olivé E, Aranda MA, Gosálvez B, Castillo P, et al. First detection of tomato leaf curl New Delhi virus infecting Zucchini in Spain. Plant Dis. 2014;98(6):857. https://doi.org/10.1094/PDIS-10-13-1050-PDN PMID: 30708660
6. Ruiz ML, Simón A, Velasco L, García MC, Janssen D. First report of tomato leaf curl New Delhi virus infecting tomato in Spain. Plant Dis. 2015;99(6):894–894. https://doi.org/10.1094/pdis-10-14-1072-pdn
7. Panno S, Caruso AG, Troiano E, Luigi M, Manglli A, Vatrano T, et al. Emergence of tomato leaf curl New Delhi virus in Italy: estimation of incidence and genetic diversity. Plant Pathol. 2019;68(3):601–8. https://doi.org/10.1111/ppa.12978
8. Fondong VN. Geminivirus protein structure and function. Mol Plant Pathol. 2013;14(6):635–49. https://doi.org/10.1111/mpp.12032 PMID: 23615043
9. Hanley-Bowdoin L, Bejarano ER, Robertson D, Mansoor S. Geminiviruses: masters at redirecting and reprogramming plant processes. Nat Rev Microbiol. 2013;11(11):777–88. https://doi.org/10.1038/nrmicro3117 PMID: 24100361
10. Briddon RW, Stanley J. Subviral agents associated with plant single-stranded DNA viruses. Virology. 2006;344(1):198–210. https://doi.org/10.1016/j.virol.2005.09.042 PMID: 16364750
11. Saunders K, Norman A, Gucciardo S, Stanley J. The DNA beta satellite component associated with ageratum yellow vein disease encodes an essential pathogenicity protein (betaC1). Virology. 2004;324(1):37–47. https://doi.org/10.1016/j.virol.2004.03.018 PMID: 15183051
12. Jose J, Usha R. Bhendi yellow vein mosaic disease in India is caused by association of a DNA Beta satellite with a begomovirus. Virology. 2003;305(2):310–7. https://doi.org/10.1006/viro.2002.1768 PMID: 12573576
13. Briddon RW, Mansoor S, Bedford ID, Pinner MS, Saunders K, Stanley J, et al. Identification of dna components required for induction of cotton leaf curl disease. Virology. 2001;285(2):234–43. https://doi.org/10.1006/viro.2001.0949 PMID: 11437658
14. Hu T, Song Y, Wang Y, Zhou X. Functional analysis of a novel βV1 gene identified in a geminivirus betasatellite. Sci China Life Sci. 2020;63(5):688–96. https://doi.org/10.1007/s11427-020-1654-x PMID: 32107688
15. Gupta N, Reddy K, Gnanasekaran P, Zhai Y, Chakraborty S, Pappu HR. Functional characterization of a new ORF βV1 encoded by radish leaf curl betasatellite. Front Plant Sci. 2022;13:972386. https://doi.org/10.3389/fpls.2022.972386 PMID: 36212370
16. Amin I, Patil BL, Briddon RW, Mansoor S, Fauquet CM. A common set of developmental miRNAs are upregulated in Nicotiana benthamiana by diverse begomoviruses. Virol J. 2011;8:143. https://doi.org/10.1186/1743-422X-8-143 PMID: 21447165
17. Zhong X, Wang ZQ, Xiao R, Cao L, Wang Y, Xie Y, et al. Mimic phosphorylation of a βC1 protein encoded by TYLCCNB impairs its functions as a viral suppressor of RNA silencing and a symptom determinant. J Virol. 2017;91(16):e00300–17. https://doi.org/10.1128/JVI.00300-17 PMID: 28539450
18. Zhou X, Huang C. Virus-induced gene silencing using begomovirus satellite molecules. In: Watson JM, Wang MB, editors. Antiviral resistance in plants. Humana Press; 2012. pp. 57–67.
19. Bhattacharyya D, Gnanasekaran P, Kumar RK, Kushwaha NK, Sharma VK. A geminivirus betasatellite damages the structural and functional integrity of chloroplasts leading to symptom formation and inhibition of photosynthesis. J Exp Bot. 2015;66:5881–95.
20. Cui X, Li G, Wang D, Hu D, Zhou X. A Begomovirus DNAbeta-encoded protein binds DNA, functions as a suppressor of RNA silencing, and targets the cell nucleus. J Virol. 2005;79(16):10764–75. https://doi.org/10.1128/JVI.79.16.10764-10775.2005 PMID: 16051868

21. Gnanasekaran P, Ponnusamy K, Chakraborty S. A geminivirus betasatellite encoded βC1 protein interacts with PsbP and subverts PsbP-mediated antiviral defence in plants. Mol Plant Pathol. 2019;20(7):943–60. https://doi.org/10.1111/mpp.12804 PMID: 30985068
22. Kamal H, Minhas F-U-AA, Farooq M, Tripathi D, Hamza M, Mustafa R, et al. In silico Prediction and validations of domains involved in *Gossypium hirsutum* SnRK1 protein interaction with cotton leaf curl multan betasatellite encoded βC1. Front Plant Sci. 2019;10:656. https://doi.org/10.3389/fpls.2019.00656 PMID: 31191577
23. Eini O, Dogra S, Selth LA, Dry IB, Randles JW, Rezaian MA. Interaction with a host ubiquitin-conjugating enzyme is required for the pathogenicity of a geminiviral DNA beta satellite. Mol Plant Microbe Interact. 2009;22(6):737–46. https://doi.org/10.1094/MPMI-22-6-0737 PMID: 19445598
24. Gnanasekaran P, Gupta N, Ponnusamy K, Chakraborty S. Geminivirus betasatellite-encoded βC1 protein exhibits novel ATP hydrolysis activity that influences its DNA-binding activity and viral pathogenesis. J Virol. 2021;95(17):e0047521. https://doi.org/10.1128/JVI.00475-21 PMID: 34132576
25. Zhang T, Luan J-B, Qi J-F, Huang C-J, Li M, Zhou X-P, et al. Begomovirus-whitefly mutualism is achieved through repression of plant defences by a virus pathogenicity factor. Mol Ecol. 2012;21(5):1294–304. https://doi.org/10.1111/j.1365-294X.2012.05457.x PMID: 22269032
26. Ilyas M, Qazi J, Mansoor S, Briddon RW. Genetic diversity and phylogeography of begomoviruses infecting legumes in Pakistan. J Gen Virol. 2010;91(Pt 8):2091–101. https://doi.org/10.1099/vir.0.020404-0 PMID: 20375225
27. Qazi J, Ilyas M, Mansoor S, Briddon RW. Legume yellow mosaic viruses: genetically isolated begomoviruses. Mol Plant Pathol. 2007;8(4):343–8. https://doi.org/10.1111/j.1364-3703.2007.00402.x PMID: 20507504
28. Rouhibakhsh A, Malathi VG. Severe leaf curl disease of cowpea – a new disease of cowpea in northern India caused by *Mungbean yellow mosaic India virus* and a satellite DNA β. Plant Pathology. 2005;54(2):259–259. https://doi.org/10.1111/j.1365-3059.2005.01139.x
29. Guo W, Yang X, Xie Y, Cui X, Zhou X. Tomato yellow leaf curl Thailand virus-[Y72] from Yunnan is a monopartite begomovirus associated with DNAbeta. Virus Genes. 2009;38(2):328–33. https://doi.org/10.1007/s11262-009-0327-4 PMID: 19165588
30. Sivalingam PN, Malathi VG, Varma A. Molecular diversity of the DNA-beta satellites associated with tomato leaf curl disease in India. Arch Virol. 2010;155(5):757–64. https://doi.org/10.1007/s00705-010-0634-z PMID: 20229326
31. Jyothsna P, Haq QMI, Singh P, Sumiya KV, Praveen S, Rawat R, et al. Infection of tomato leaf curl New Delhi virus (ToLCNDV), a bipartite begomovirus with betasatellites, results in enhanced level of helper virus components and antagonistic interaction between DNA B and betasatellites. Appl Microbiol Biotechnol. 2013;97(12):5457–71. https://doi.org/10.1007/s00253-012-4685-9 PMID: 23306645
32. Akhter A, Akhtar S, Saeed M, Mansoor S. Chili leaf curl betasatellite enhances symptoms induced by tomato leaf curl New Delhi virus, a bipartite begomovirus. Int J Agric Biol. 2014;16:1225–8.
33. Agnihotri AK, Mishra SP, Tripathi RC, Ansar M, Srivastava A, Tripathi IP. First natural co-occurrence of tomato leaf curl New Delhi virus DNA-A and chili leaf curl betasatellite on tomato plants (*Solanum lycopersicum* L.) in India. J Gen Plant Pathol. 2018;84(6):414–7. https://doi.org/10.1007/s10327-018-0807-2
34. Hameed A, Tahir MN, Amin I, Mansoor S. First report of tomato leaf curl New Delhi virus and a tomato yellow leaf curl Thailand betasatellite causing severe leaf curl disease of potato in Pakistan. Plant Dis. 2017;101(6):1065–1065. https://doi.org/10.1094/pdis-09-16-1335-pdn
35. Anwar S. Distinct association of an alphasatellite and a betasatellite with tomato leaf curl New Delhi virus in field-infected cucurbit. J Gen Plant Pathol. 2017;83(3):185–8. https://doi.org/10.1007/s10327-017-0709-8
36. Venkataravanappa V, Reddy CNL, Shankarappa KS, Reddy MK. Association of Tomato Leaf Curl New Delhi Virus, Betasatellite, and Alphasatellite with Mosaic Disease of Spine Gourd (*Momordica dioica* Roxb. Willd) in India. Iran J Biotechnol. 2019;17(1):e2134. https://doi.org/10.21859/ijb.2134 PMID: 31457044
37. Shahid MS, Mansoor S, Brown JK, Briddon RW. Interaction of a tomato leaf curl New Delhi virus with a betasatellite enhances symptom severity in field-infected tomato plants. Trop Plant Pathol. 2021;46(2):169–74. https://doi.org/10.1007/s40858-020-00414-0
38. Vignesh S, Renukadevi P, Nagendran K, Senthil N, Kumar RV, SwarnaPriya R, et al. A distinct strain of tomato leaf curl New Delhi virus that causes mosaic disease in ash gourd and other cucurbitaceous crops. Front Microbiol. 2023;14:1268333. https://doi.org/10.3389/fmicb.2023.1268333 PMID: 37965544
39. Iqbal Z, Shafiq M, Ali I, Mansoor S, Briddon RW. Maintenance of cotton leaf curl multan betasatellite by tomato leaf curl New Delhi virus-analysis by mutation. Front Plant Sci. 2017;8:2208. https://doi.org/10.3389/fpls.2017.02208 PMID: 29312431
40. Iqbal Z, Shafiq M, Briddon RW. Cotton leaf curl Multan betasatellite impaired ToLCNDV ability to maintain cotton leaf curl Multan alphasatellite. Braz J Biol. 2022;84:e260922. https://doi.org/10.1590/1519-6984.260922 PMID: 35894353
41. Ranjan P, Singh AK, Kumar RV, Basu S, Chakraborty S. Host-specific adaptation of diverse betasatellites associated with distinct Indian tomato-infecting begomoviruses. Virus Genes. 2014;48(2):334–42. https://doi.org/10.1007/s11262-013-1031-y PMID: 24384936
42. Singh AK, Kushwaha N, Chakraborty S. Synergistic interaction among begomoviruses leads to the suppression of host defense-related gene expression and breakdown of resistance in chilli. Appl Microbiol Biotechnol. 2016;100(9):4035–49. https://doi.org/10.1007/s00253-015-7279-5 PMID: 26780359
43. Hussain T, Ali M. A review of cotton diseases of Pakistan. Pakistan Cotton. 1975;19:71–86.
44. Briddon RW, Markham PG. Cotton leaf curl virus disease. Virus Res. 2000;71(1–2):151–9. https://doi.org/10.1016/s0168-1702(00)00195-7 PMID: 11137169

45. Mansoor S, Amin I, Iram S, Hussain M, Zafar Y, Malik KA, et al. Breakdown of resistance in cotton to cotton leaf curl disease in Pakistan. Plant Pathol. 2003;52(6):784–784. https://doi.org/10.1111/j.1365-3059.2003.00893.x
46. Amrao L, Akhter S, Tahir MN, Amin I, Briddon RW, Mansoor S. Cotton leaf curl disease in Sindh province of Pakistan is associated with recombinant begomovirus components. Virus Res. 2010;153(1):161–5. https://doi.org/10.1016/j.virusres.2010.07.003 PMID: 20621137
47. Zubair M, Zaidi SS-E-A, Shakir S, Farooq M, Amin I, Scheffler JA, et al. Multiple begomoviruses found associated with cotton leaf curl disease in Pakistan in early 1990 are back in cultivated cotton. Sci Rep. 2017;7(1):680. https://doi.org/10.1038/s41598-017-00727-2 PMID: 28386113
48. Datta S, Budhauliya R, Das B, Gopalakrishnan R, Sharma S. Rebound of cotton leaf curl Multan virus and its exclusive detection in cotton leaf curl disease outbreak, Punjab (India), 2015. Sci Rep. 2017;7:17361.
49. Zaidi SS-E-A, Martin DP, Amin I, Farooq M, Mansoor S. Tomato leaf curl New Delhi virus: a widespread bipartite begomovirus in the territory of monopartite begomoviruses. Mol Plant Pathol. 2017;18(7):901–11. https://doi.org/10.1111/mpp.12481 PMID: 27553982
50. Biswas KK, Balram N, Elangovan M, Palchoudhury S, Bhattacharyya UK, Khatoon H, et al. Divergent Cotton leaf curl Multan betasatellite and three different alphasatellite species associated with cotton leaf curl disease outbreak in Northwest India. PLoS One. 2025;20(1):e0313844. https://doi.org/10.1371/journal.pone.0313844 PMID: 39787193
51. Iqbal Z, Sattar MN, Kvarnheden A, Mansoor S, Briddon RW. Effects of the mutation of selected genes of *cotton leaf curl Kokhran virus* on infectivity, symptoms and the maintenance of cotton leaf curl Multan betasatellite. Virus Res. 2012;169(1):107–16. https://doi.org/10.1016/j.virusres.2012.07.016 PMID: 22871297
52. Tamura K, Stecher G, Peterson D, Filipski A, Kumar S. MEGA6: Molecular Evolutionary Genetics Analysis version 6.0. Mol Biol Evol. 2013;30:2725–9.
53. Ilyas M, Qazi J, Mansoor S, Briddon RW. Molecular characterisation and infectivity of a "Legumovirus" (genus *Begomovirus*: family *Geminiviridae*) infecting the leguminous weed *Rhynchosia minima* in Pakistan. Virus Res. 2009;145(2):279–84. https://doi.org/10.1016/j.virusres.2009.07.018 PMID: 19664665
54. Doyle JJ, Doyle JL (1987) A rapid DNA isolation procedure for small quantities of fresh leaf tissue. Phytochem Bull. 19: 11–5.
55. Sambrook J, Frisch EF, Maniatis T. Molecular Cloning: A Laboratory Manual. New York: Cold Spring Harbor Laboratory Press; 1989.
56. Schneider CA, Rasband WS, Eliceiri KW. NIH Image to ImageJ: 25 years of image analysis. Nat Methods. 2012;9(7):671–5. https://doi.org/10.1038/nmeth.2089 PMID: 22930834
57. Shafiq M, Iqbal Z, Ali I, Abbas Q, Mansoor S, Briddon RW, et al. Real-time quantitative PCR assay for the quantification of virus and satellites causing leaf curl disease in cotton in Pakistan. J Virol Methods. 2017;248:54–60. https://doi.org/10.1016/j.jviromet.2017.05.012 PMID: 28572041
58. Iqbal Z, Shafiq M, Ali S, Mahmood MA, Siddiqui HA, Amin I, et al. qPCR assay as a tool for examining cotton resistance to the virus complex causing CLCuD: yield loss inversely correlates with betasatellite, not virus, DNA Titer. Plants (Basel). 2023;12(14):2645. https://doi.org/10.3390/plants12142645 PMID: 37514259
59. Yan Y, Zhang D, Zhou P, Li B, Huang S-Y. HDOCK: a web server for protein-protein and protein-DNA/RNA docking based on a hybrid strategy. Nucleic Acids Res. 2017;45(W1):W365–73. https://doi.org/10.1093/nar/gkx407 PMID: 28521030
60. Bull SE, Tsai W-S, Briddon RW, Markham PG, Stanley J, Green SK. Diversity of begomovirus DNA beta satellites of non-malvaceous plants in east and south east Asia. Arch Virol. 2004;149(6):1193–200. https://doi.org/10.1007/s00705-003-0282-7 PMID: 15168205
61. Zaidi SS-E-A, Shafiq M, Amin I, Scheffler BE, Scheffler JA, Briddon RW, et al. Frequent occurrence of *tomato leaf curl New Delhi virus* in cotton leaf curl disease affected cotton in Pakistan. PLoS One. 2016;11(5):e0155520. https://doi.org/10.1371/journal.pone.0155520 PMID: 27213535
62. Briddon RW, Bull SE, Amin I, Idris AM, Mansoor S, Bedford ID, et al. Diversity of DNA beta, a satellite molecule associated with some monopartite begomoviruses. Virology. 2003;312(1):106–21. https://doi.org/10.1016/s0042-6822(03)00200-9 PMID: 12890625
63. Zhou X. Advances in understanding begomovirus satellites. Annu Rev Phytopathol. 2013;51:357–81. https://doi.org/10.1146/annurev-phyto-082712-102234 PMID: 23915133
64. Klinkenberg FA, Stanley J. Encapsidation and spread of African cassava mosaic virus DNA A in the absence of DNA B when agroinoculated to *Nicotiana benthamiana*. J Gen Virol. 1990;71(6):1409–12. https://doi.org/10.1099/0022-1317-71-6-1409
65. Evans D, Jeske H. DNA B facilitates, but is not essential for, the spread of abutilon mosaic virus in agroinoculated *Nicotiana benthamiana*. Virology. 1993;194(2):752–7. https://doi.org/10.1006/viro.1993.1316 PMID: 8503185
66. Pratap D, Kashikar AR, Mukherjee SK. Molecular characterization and infectivity of a Tomato leaf curl New Delhi virus variant associated with newly emerging yellow mosaic disease of eggplant in India. Virol J. 2011;8:305. https://doi.org/10.1186/1743-422X-8-305 PMID: 21676270
67. Li F, Wang Y, Zhou X. SGS3 Cooperates with RDR6 in Triggering Geminivirus-Induced Gene Silencing and in Suppressing Geminivirus Infection in *Nicotiana Benthamiana*. Viruses. 2017;9(9):247. https://doi.org/10.3390/v9090247 PMID: 28869553
68. Akhter A, Qazi J, Saeed M, Mansoor S. A severe leaf curl disease on Chilies in Pakistan is associated with multiple Begomovirus components. Plant Dis. 2009;93(9):962. https://doi.org/10.1094/PDIS-93-9-0962B PMID: 30754557
69. Saunders K, Bedford ID, Briddon RW, Markham PG, Wong SM, Stanley J. A unique virus complex causes *Ageratum* yellow vein disease. Proc Natl Acad Sci U S A. 2000;97(12):6890–5. https://doi.org/10.1073/pnas.97.12.6890 PMID: 10841581
70. Sattar MN. *In planta* interaction and transreplication of distinct begomoviruses and their associated components. Int J Agric Biol. 2021;26(01):45–51. https://doi.org/10.17957/ijab/15.1807

71. Sanderfoot AA, Lazarowitz SG. Cooperation in viral movement: the geminivirus BL1 movement protein interacts with BR1 and redirects it from the nucleus to the cell periphery. Plant Cell. 1995;7(8):1185–94. https://doi.org/10.1105/tpc.7.8.1185 PMID: 12242403

72. Sanderfoot AA, Lazarowitz SG. Getting it together in plant virus movement: cooperative interactions between bipartite geminivirus movement proteins. Trends Cell Biol. 1996;6(9):353–8. https://doi.org/10.1016/0962-8924(96)10031-3 PMID: 15157433

73. Saeed M. The role of geminiviral DNA b satellite in viral pathogenicity and movement. Faisalabad: University of Agriculture; 2007. pp. 84.

74. Yin Y, Beachy RN. The regulatory regions of the rice tungro bacilliform virus promoter and interacting nuclear factors in rice (*Oryza sativa* L.). Plant J. 1995;7(6):969–80. https://doi.org/10.1046/j.1365-313x.1995.07060969.x PMID: 7599653

75. Eini O, Behjatnia SAA, Dogra S, Dry IB, Randles JW, Rezaian MA. Identification of sequence elements regulating promoter activity and replication of a monopartite begomovirus-associated DNA beta satellite. J Gen Virol. 2009;90(Pt 1):253–60. https://doi.org/10.1099/vir.0.002980-0 PMID: 19088296

76. Li D, Behjatnia SAA, Dry IB, Randles JW, Eini O, Rezaian MA. Genomic regions of tomato leaf curl virus DNA satellite required for replication and for satellite-mediated delivery of heterologous DNAs. J Gen Virol. 2007;88(Pt 7):2073–7. https://doi.org/10.1099/vir.0.82853-0 PMID: 17554042

77. Reddy K, Bhattacharyya D, Chakraborty S. Mutational study of radish leaf curl betasatellite to understand the role of the non-coding region in begomovirus pathogenesis. Physiol Mol Plant Pathol. 2020;112:101549. https://doi.org/10.1016/j.pmpp.2020.101549

78. Amrao L, Amin I, Shahid MS, Briddon RW, Mansoor S. Cotton leaf curl disease in resistant cotton is associated with a single begomovirus that lacks an intact transcriptional activator protein. Virus Res. 2010;152(1–2):153–63. https://doi.org/10.1016/j.virusres.2010.06.019 PMID: 20600387

79. Amin I, Mansoor S, Amrao L, Hussain M, Irum S, Zafar Y, et al. Mobilisation into cotton and spread of a recombinant cotton leaf curl disease satellite. Arch Virol. 2006;151(10):2055–65. https://doi.org/10.1007/s00705-006-0773-4 PMID: 16732497

80. Akhtar S, Khan AJ, Singh AS, Briddon RW. Identification of a disease complex involving a novel monopartite begomovirus with beta- and alpha-satellites associated with okra leaf curl disease in Oman. Arch Virol. 2014;159(5):1199–205. https://doi.org/10.1007/s00705-013-1926-x PMID: 24287711

81. Qazi J, Amin I, Mansoor S, Iqbal MJ, Briddon RW. Contribution of the satellite encoded gene betaC1 to cotton leaf curl disease symptoms. Virus Res. 2007;128(1–2):135–9. https://doi.org/10.1016/j.virusres.2007.04.002 PMID: 17482706

82. Xu X, Qian Y, Wang Y, Li Z, Zhou X. Iterons homologous to helper geminiviruses are essential for efficient replication of betasatellites. J Virol. 2019;93(5):e01532-18. https://doi.org/10.1128/JVI.01532-18 PMID: 30541843

83. Kumar P P, Usha R, Zrachya A, Levy Y, Spanov H, Gafni Y. Protein-protein interactions and nuclear trafficking of coat protein and betaC1 protein associated with Bhendi yellow vein mosaic disease. Virus Res. 2006;122(1–2):127–36. https://doi.org/10.1016/j.virusres.2006.07.007 PMID: 16934356

84. Gnanasekaran P, KishoreKumar R, Bhattacharyya D, Vinoth Kumar R, Chakraborty S. Multifaceted role of geminivirus associated betasatellite in pathogenesis. Mol Plant Pathol. 2019;20(7):1019–33. https://doi.org/10.1111/mpp.12800 PMID: 31210029

85. Namrata J, Saritha RK, Datta D, Singh M, Dubey RS, Rai AB, et al. Molecular Characterization of Tomato leaf curl Palampur virus and Pepper leaf curl betasatellite Naturally Infecting Pumpkin (Cucurbita moschata) in India. Indian J Virol. 2010;21(2):128–32. https://doi.org/10.1007/s13337-011-0022-7 PMID: 23637491

86. Sattar MN, Khurshid M, El-Beltagi HS, Iqbal Z. Identification and estimation of sequence variation dynamics of Tomato Leaf curl Palampur virus and betasatellite complex infecting a new weed host. Biotechnol Biotechnol Equip. 2022;36(1):609–19. https://doi.org/10.1080/13102818.2022.2112911

87. Sharma D, Kulshreshtha A, Roshan P, Hallan V. Molecular characterization and infectivity analysis of a bipartite begomovirus associated with cotton leaf curl Multan betasatellite naturally infecting Rumex nepalensis in northern India. J Plant Pathol. 2019;101(4):935–41. https://doi.org/10.1007/s42161-019-00295-6